Characterization of Ultrathin Films of γ-Al_2O_3 and the Chemistry of 1,3-Butadiene on NiAl(001) and γ-Al_2O_3

Michelle M. Ivey, Kathryn A. Layman, Armen Avoyan, Heather C. Allen,† and John C. Hemminger*

Department of Chemistry and Institute for Surface and Interface Science, University of California, Irvine, Irvine, California 92697

Received: October 3, 2002; In Final Form: March 27, 2003

Ultrathin films of γ-Al_2O_3 grown on NiAl(001) were studied using high-resolution electron energy loss spectroscopy (HREELS), Auger electron spectroscopy (AES), and low-energy electron diffraction (LEED). Growth of the ultrathin oxide films with water produces a hydroxylated surface, as confirmed by vibrational spectroscopy. Also, exposure of a film grown with O_2, to H_2O following growth results in OH groups on the surface. Following adsorption at 170 K, the OH-stretching mode is observed (HREELS) as a relatively narrow band at 3690 cm^{-1} with a broad, low-intensity shoulder to lower frequencies, indicative of isolated OH groups bridge-bonded to aluminum sites and a small degree of OH hydrogen-bonding. The hydrogen-bonded species are removed by warming above 210 K. Adsorption and reaction of 1,3-butadiene on NiAl(001), and thin films of γ-Al_2O_3, have been studied using HREELS, laser-induced desorption coupled with Fourier transform mass spectroscopy (LID-FTMS), AES, and LEED. We find that at 170 K, the 1,3-butadiene is irreversibly π-bonded to NiAl(001). Upon warming the surface to 300 K, the adsorbate is efficiently converted into σ-bonded species without undergoing decomposition, and is stable within the 300−400 K temperature range. Heating the surface above 400 K causes decomposition of the adsorbate. In contrast, the 1,3-butadiene adsorption on thin films of both hydroxylated and non-hydroxylated γ-Al_2O_3 is largely reversible. Dimerization of 1,3-butadiene to 4-vinylcyclohexene was observed on hydroxylated γ-Al_2O_3. Some decomposition of the 1,3-butadiene takes place on both oxide surfaces at temperatures as low as 170 K.

1. Introduction

Metal oxides play a large role as catalysts and catalyst supports. While these systems are in widespread use, the detailed chemical mechanisms are not always well understood. Aluminum oxide is used extensively as a support for metal catalysts, as a component in chromatographic columns, and is present as particles in the stratosphere and troposphere. In our studies, we utilize surface-specific probes of thin films of aluminum oxide in an effort to better understand the chemistry occurring in these systems.

Aluminum oxide can exist in a number of phases, all of which consist of a close packed oxygen lattice with aluminum cations occupying tetrahedral and/or octahedral vacancies. The most stable phase is α-alumina, which has a hexagonal closest-packed oxygen sub-lattice with aluminum atoms occupying octahedral vacancies. γ-Alumina is a metastable phase, which can be converted to α-alumina upon heating to 1473 K. γ-Alumina has a face-centered cubic oxygen sub-lattice with aluminum atoms occupying both octahedral and tetrahedral sites. γ-Alumina is used extensively as a catalyst[1−6] and a catalytic support.[7−9] The electron scattering techniques utilized in our experiments require preparation of thin films (≤10 Å) of γ-Al_2O_3 due to the insulating nature of the bulk material. Also, γ-Al_2O_3 is not available in large single crystals, so thin films on a conducting substrate is a good alternative to powdered samples.

Consequently, the first stage of our research was devoted to synthesis and characterization of thin films of γ-Al_2O_3. The choice of the substrate is not incidental, since Gassmann et al.[10] have shown that the phase of the thin well-ordered alumina grown on NiAl(001) can be controlled by varying the thermal regime of the sample and partial pressure of the O_2 exposure during oxidation. In the presence of oxygen, the films grow at elevated temperatures by outward diffusion of Al atoms from the bulk. From the attenuation of the Ni(848) Auger electron spectroscopy (AES) transition, Gassmann et al.[10] have estimated the thickness of the self-limited oxide film grown at 1200 K to be 8 Å ± 2.5 Å. The saturation level of the surface oxide, corresponding to an AES O(505)/Ni(848) ratio of 2.5, was obtained by a 2400 L O_2 exposure at 1300 K.[10] Blum et al. studied the initial growth of Al_2O_3 on NiAl(001) and found that the surface consisted of elongated oxide stripes along the ⟨100⟩ and ⟨010⟩ directions of the NiAl(001) surface.[11] The films prepared by Gassmann et al. had no hydroxyl groups.[10] However, we found that by exposing the NiAl(001) substrate to H_2O one can grow well-ordered thin films of hydroxylated γ-alumina at temperatures as high as ∼1000 K.

Growing Al_2O_3 on NiAl(001) is not the only way to produce thin films of alumina on a conducting substrate. NiAl(110) has also been used by others to produce well-ordered thin films of Al_2O_3 ∼5 Å thick.[12−15] Libuda et al. modified the surface to form hydroxyl groups by evaporating metallic Al and subsequent water exposure.[14] Substrates other than NiAl have also been used. Becker et al. showed that thin films of γ-aluminum oxide could be formed by oxidizing the $Ni_3Al(111)$ surface.[16] Another

* Corresponding author. Phone: (949) 824-6020. Fax: (949) 824-3168. E-mail: jchemmin@uci.edu.

† Present address: Department of Chemistry, Ohio State University, 100 W. 18th Ave., Columbus, OH.

10.1021/jp022177g CCC: $25.00
Published on Web 06/10/2003

method is to oxidize the Al(111) surface.[17] Aluminum has been deposited with an oxygen atmosphere onto substrates such as Mo(110),[18,19] Ta(110),[20] Ru(0001),[21] and Re(0001).[21,22] We have chosen to oxidize the NiAl(001) surface because this substrate yields ~10 Å thick (somewhat thicker than that obtained on NiAl(110)), well-ordered films and offers the flexibility of obtaining different phases of alumina, depending on the oxidation conditions.[10]

In this manuscript we also describe the chemistry of 1,3-butadiene on clean NiAl(001) and thin films of γ-alumina. We are interested in the chemistry of butadiene on aluminum oxide for several reasons. Al_2O_3 is a component of soil-derived dust particles. Butadiene is an industrial emission gas and has recently been identified as a carcinogen.[23,24] These dust particles may provide a surface for butadiene to form products which are either more or less toxic than the parent compound. Alternatively, the particles themselves could play a role in introducing the toxin into the lungs. The chemistry of butadiene on aluminum oxide also provides us with a probe of the catalytic properties of alumina, and in particular the difference between hydroxylated and non-hydroxylated surfaces.

We found that 1,3-butadiene adsorption on clean NiAl(001) at 170 K is irreversible. At this temperature it is π-bonded to the substrate and no multilayer condensation of 1,3-butadiene was observed. Warming the surface to 300 K leads to very efficient conversion of π-bonded butadiene into a σ-bonded species, which is thermally stable below 400 K. Heating the surface above 400 K results in decomposition of the butadiene. The 1,3-butadiene adsorption on thin films of both hydroxylated and non-hydroxylated γ-Al_2O_3 is largely reversible. Laser-induced desorption Fourier transform mass spectrometry (LID-FTMS) experiments indicate that 1,3-butadiene dimerizes to form 4-vinylcyclohexene on hydroxylated γ-Al_2O_3, but there is no reaction on the non-hydroxylated surface. Vibrational spectroscopy shows that there is a small amount of dehydrogenation of 1,3-butadiene on both hydroxylated and non-hydroxylated γ-Al_2O_3 at temperatures as low as 170 K.

2. Experimental Section

The HREELS experiments were carried out in an ion-pumped UHV chamber that has a base pressure of $\sim 1 \times 10^{-10}$ Torr. The chamber is equipped with a single-pass cylindrical mirror analyzer (Physical Electronics 10-155) with a coaxial electron gun for Auger electron spectroscopy (AES) analysis, a UTI-100C quadrupole mass spectrometer for residual gas analysis, Varian low-energy electron diffraction (LEED) optics, an LK-2000 high-resolution electron energy loss spectrometer (HREELS), and an ion gun for ion bombardment.

A 3 kV/1 μA electron beam was employed for AES analysis. Typical HREELS conditions were as follow: a 7 eV kinetic energy incident beam, resolution of ~5−8 meV, and count rates ~100 kHz in the elastic, and ~1−10 kHz in inelastic channels. All HREEL spectra presented here were recorded at 170 K. The period of signal averaging was kept at ~2 h per spectrum in order to minimize the influence of background contamination. Each HREELS spectrum was normalized with respect to its own elastic peak, and the corresponding number of scans.

The LID-FTMS experiments were carried out in a separate ion-pumped UHV chamber with a base pressure of $\sim 5 \times 10^{-10}$ Torr. The chamber is equipped with a single-pass cylindrical mirror analyzer (Physical Electronics 10-155) equipped with an electron gun for AES analysis, PHI LEED optics, and an ion gun for ion bombardment. In a typical LID-FTMS experiment, a 0.5 mm × 1 mm spot is irradiated with a pulsed laser (KrF excimer laser, 248 nm, 20 ns pulse width), which causes such a rapid temperature jump that the molecules desorb intact, even if slower heating rates would have resulted in a surface reaction.[25−28] The neutral molecules are then ionized by electron ionization (70 eV) and detected by Fourier transform mass spectrometry.[25] The laser optics are controlled such that each laser pulse probes a different spot on the surface.

NiAl(001) samples were prepared from a 1 cm diameter single-crystal rod of NiAl, obtained from GE Research Labs (Schnectady, New York). Slices of 2 mm thickness were cut by an electric discharge machine (California Wire EDM), and both sides were polished by using standard procedures.[29] Angular misalignment of the NiAl(001) surface, examined by the Laue X-ray diffraction, did not exceed ~2°. The sample was mounted on a liquid nitrogen-cooled manipulator, equipped with resistive heating. A chromel/alumel thermocouple was spot-welded to the side of the crystal. Initially, the sample was subjected to room-temperature Ar^+ sputtering for 5 min, followed by annealing to ~1300−1400 K, to regain the crystalline structure. Thereafter, it was cleaned by cycles of O_2 thermal treatment at $p_{O_2} = 1.0-2.0 \times 10^{-7}$ Torr and ~1000 K for 2 min, followed by flashing the surface to ~1500 K. The cleanliness and surface composition of the substrate were monitored by AES and LEED. Carbon and oxygen, the primary surface contaminants, are readily removed by several cleaning cycles

The 1,3-butadiene (C_4H_6) (Aldrich Chemical Co., Inc., 99+%) was used without further purification. The 18 MΩ deionized H_2O, and D_2O (99.996% isotopic enrichment, Cambridge Isotope Laboratories, 98+%) were de-gassed by freeze, pump, and thaw cycles. The cleanliness of all gases introduced into the chamber was checked in situ by mass spectrometry.

Thin films of non-hydroxylated and hydroxylated γ-Al_2O_3, used throughout the experiments, and characterized by AES, LEED, and HREELS, were prepared by exposing the NiAl-(001) substrate to O_2 or H_2O at ~1000 K. The Auger O(505)/Ni(848) ratio = 2.5−3.0 was defined as a saturation coverage of γ-Al_2O_3 at the preparation temperature of ~1000 K. This ratio was obtainable by either a 2400 L O_2, or a ~100 L H_2O exposure (1 L = 1×10^{-6} Torr × s). The Auger spectra of the films used in our experiments are comparable to those of films grown by Gassman et al. which were estimated to be ~10Å thick. [10,30] Previous experiments on such films indicate that they are good models of alumina surfaces and that the subsequent chemistry is not effected by the substrate. [15] Hydroxylated surfaces could also be produced by exposing a non-hydroxylated γ-Al_2O_3 thin film (grown from O_2 exposure) to exposures of ≤100 L water. When preparing γ-Al_2O_3 films for HREELS experiments, the background pressure in the chamber during the exposure did not exceed $p_{O_2} = 2.0 \times 10^{-7}$ Torr, and $p_{H_2O} = 1.0 \times 10^{-8}$ Torr, respectively. In the HREELS chamber, all exposures were only corrected for the doser flux enhancement of ×50. For the LID-FTMS experiments, the oxide layer was grown at an oxygen exposure of 1500 L at 930 K where the background oxygen pressure was 2.0×10^{-7} Torr. Hydroxylated surfaces were prepared by exposing a non-hydroxylated surface to 1 L of water at 300 K. In the LID-FTMS chamber, all exposures were corrected only for a doser flux enhancement of ×100.

3. Results and Discussion

3.1. Synthesis and Characterization of Thin Films of γ-Al_2O_3. Figure 1a shows a set of HREELS spectra recorded after exposing the NiAl(001) surface to 2400 L of O_2 at

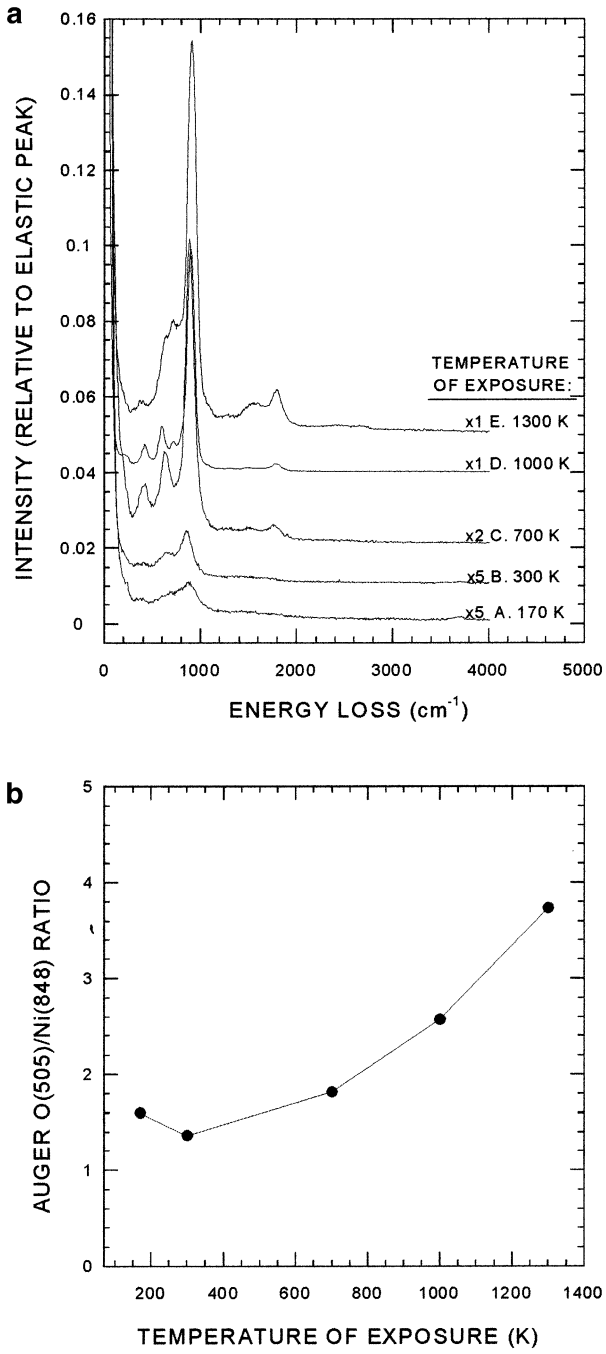

Figure 1. (a) HREELS spectra recorded after a 2400 L O_2 exposure on NiAl(001) at successively increasing temperatures. (b) Changes in surface composition as a function of increasing temperature monitored by AES.

successively increasing temperatures. Surface composition, probed by AES immediately after each HREELS spectrum, is shown in Figure 1b. The oxygen uptake by the NiAl(001) sample steadily increases with increasing exposure temperature. The HREELS spectra show that oxidation of the substrate takes place at temperatures as low as 170 K. Nonetheless, formation of well-ordered layers of alumina takes place exclusively within the 700−1000 K temperature interval. The HREELS spectra, recorded after O_2 exposure at 700 and 1000 K, display sharp phonon modes (lattice vibrations) with well-defined energies, reflecting long-range order of the synthesized thin films of alumina. The spectrum recorded after O_2 exposure at 1300 K clearly shows signs of deterioration of the quality of the alumina film, reflected in the phonon broadening.

Our results are consistent with the work of Gassmann et al.[10] who have shown that well-ordered thin layers of γ-like alumina can be grown by O_2 exposure on NiAl(001) within the 700−1300 K temperature range. They also characterized their films by AES, LEED, and HREELS. They reported a HREELS spectrum of γ-like alumina, that exhibited three sharp peaks at 410 (ν_1), 606 (ν_2), and 899 (ν_3) cm^{-1}. A new peak at 710 cm^{-1} (ν_4), observed at an O_2 exposure temperature between 1200 and 1350 K, was attributed to θ-alumina.[10] However, we noticed the appearance of a 716 cm^{-1} (ν_4) peak (along with the 416 (ν_1), 599 (ν_2), and 899 (ν_3) cm^{-1} peaks that describe the γ-Al_2O_3 surface phonon modes) at an exposure temperature as low as 1000 K. The peaks that appear on all oxide surfaces within the ~1300−1800 cm^{-1} range are due to the ($\nu_3 + \nu_1$), ($\nu_3 + \nu_2$), and ($2\nu_3$) combination/overtone bands. Off-specular measurements of surface phonon modes showed that the ν_3 mode of γ-Al_2O_3 is clearly dipole active, whereas the rest of the phonon modes are likely to be at least partially impact scattered. We refer to our films as γ-like alumina, with some admixture of θ-Al_2O_3. Both θ- and γ-Al_2O_3 have oxygen atoms in a face-centered cubic sublattice and aluminum atoms in both tetrahedral and octahedral vacancies, but the two phases differ in the arrangement of the aluminum atoms in the interstitial spaces.[31]

Figure 2a displays a set of HREELS spectra recorded after exposing the NiAl(001) sample to O_2 at 1000 K, as a function of increasing O_2 exposure. The 1000 K temperature was chosen because, as shown in Figure 1a, this temperature yields oxide films with the sharpest phonon peaks. This temperature is employed throughout our experiments for routine preparation of thin films of alumina. Figure 2b displays the surface composition monitored by AES. The HREELS spectrum recorded after a 0.3 L O_2 exposure already exhibit phonons characteristic of γ-like alumina. However, the LEED (2×1) streaking pattern that is characteristic of γ-alumina[10] is only seen at oxygen exposures of 1.2 L and above. At oxygen exposures less than 1.2 L, a LEED(c($\sqrt{2} \times 3\sqrt{2}$)R45°) pattern is observed, which has been identified by Gassman et al. as an oxygen-contaminated NiAl(100) substrate.[10] HREELS measurements of the films grown within the 1.2−12000 L oxygen exposure range exhibit more intense phonon modes corresponding to well-ordered γ-Al_2O_3. The low-frequency HREELS peak (212−234 cm^{-1}) showed some scatter in its energy as a function of the film thickness, and is most likely due to the phonon mode of the NiAl(001) substrate. The HREEL spectra recorded after the 60000 and 120000 L O_2 exposures clearly indicated that these thicker films are less than perfect, reflected in the degraded energy resolution, decreased reflectivity (decreased HREELS count rates in the elastic channel) of the oxide layer, and broadening of the phonon peaks. A noteworthy feature of the O_2 reaction on NiAl(001) is the low quality of the oxide films, grown by either high O_2 exposure (>12000 L) at 1000 K (Figure 2a), or intermediate exposures (2400 L) at high temperatures ($T = 1300$ K) (Figure 1a). Nearly identical HREELS spectra showed that both procedures had an analogous effect on the quality of the thicker oxide layers, generating films that exhibit broadened phonon spectra indicative of a higher density of defects.

On the basis of our HREELS and LEED results, the 2400 L O_2 exposure was selected for reproducible synthesis of high-quality uniform films of γ-Al_2O_3, and was employed throughout the experiments with butadiene. The HREELS showed that films prepared under these conditions have no hydroxyl groups. Auger spectra measured over a 7 mm sampling range showed that the

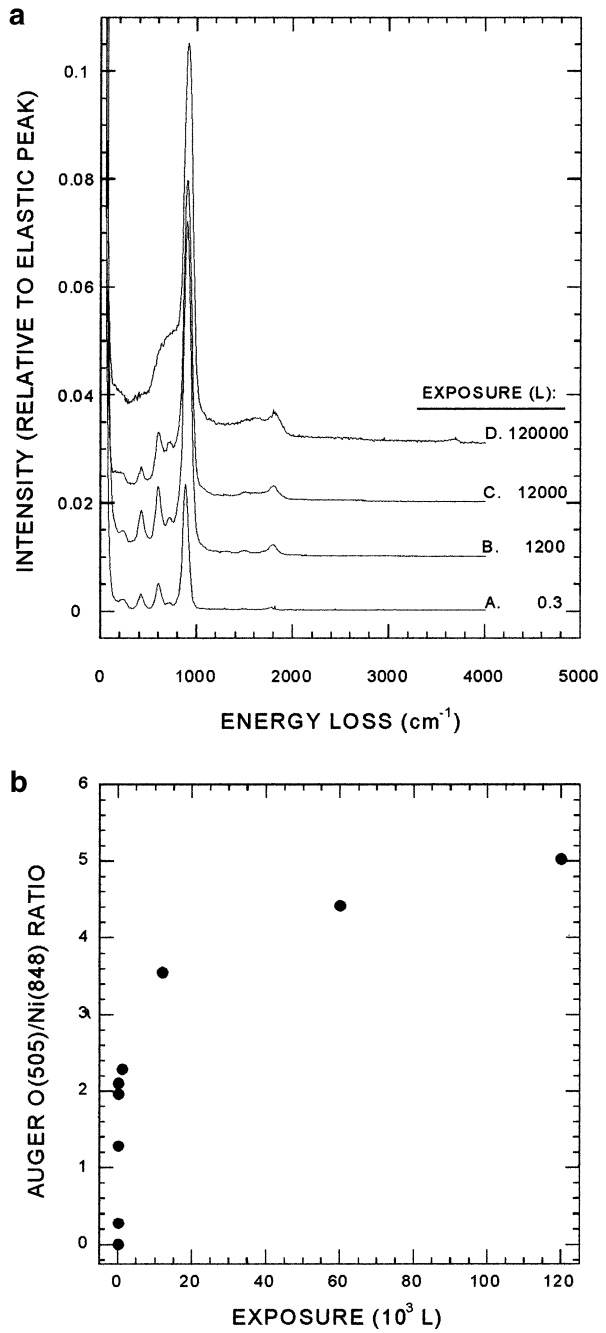

Figure 2. (a) HREELS spectra obtained after successively increasing O_2 exposures carried out on NiAl(001) at 1000 K. (b) Changes in surface composition monitored by AES.

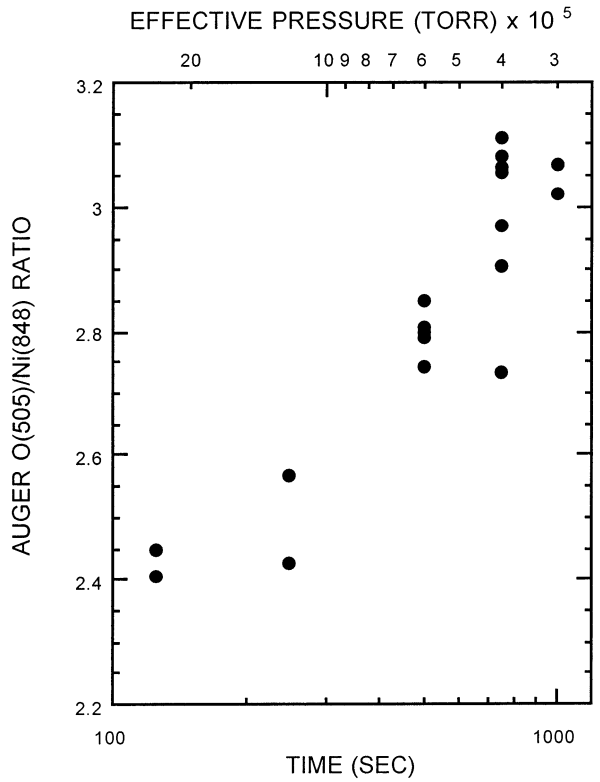

Figure 3. The Auger O(505)/Ni(848) ratio as a function of exposure time for a 30 000 L O_2 dose carried out under different pressure conditions. The longer time, lower O_2 flux growth conditions lead to thicker Al_2O_3 films for the same total exposure.

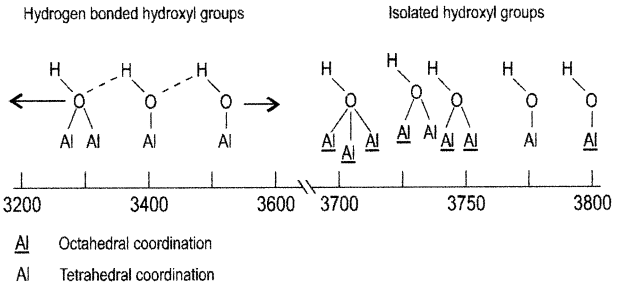

Figure 4. Diagram showing OH stretching frequencies for different types of Al_2O_3 surface sites according to Knözinger and Ratnasamy.[1] Figure adapted from Ballinger and Yates.[35]

γ-Al_2O_3 film was very uniform, exhibiting a variation of only ~5% in the O(505)/Ni(848) ratio.

In the LID-FTMS chamber, the kinetics of the aluminum oxide growth was studied using Auger electron spectroscopy. NiAl(001) was exposed to 30 000 L of oxygen (corrected for a 100× doser enhancement). This exposure was achieved under several different conditions, from exposure times of 1000 s with an effective pressure of 3×10^{-5} Torr, to 125 s with an effective pressure of 2.4×10^{-4} Torr. Figure 3 demonstrates that the oxide layer is different, depending on the oxygen flux (pressure) during growth. The oxygen-to-nickel ratio varied from 2.4 for the short exposure time to over 3 for the longer exposure time. As the oxide layer grows, aluminum atoms migrate to the surface and the nickel atoms dissolve into the bulk.[12,32] The oxide film growth is most likely limited by the Al/Ni diffusion kinetics. For the longer exposure times (lower O_2 pressures), the aluminum oxide films are thicker because the aluminum atoms have more time to migrate to the surface.

The chemistry of alumina is due to the presence of both Brønsted and Lewis acid sites on the surface. Lewis acid sites are due to coordinatively unsaturated aluminum ions. The Brønsted acid sites are due to hydroxyl groups on the surface. Knözinger and Ratnasamy identified the vibrational frequencies for the hydroxyl groups, and their assignments are shown in Figure 4. They found that hydroxyl groups close to one another exhibit stretching vibrations at low frequencies, due to hydrogen bonding between the hydroxyl groups. Five distinct isolated hydroxyl group binding sites were suggested with vibrations at higher energies. For isolated hydroxyl groups, they found that the stretching frequencies depended on how many aluminum atoms the hydroxyl group was bonded to, as well as the coordination of the underlying aluminum atoms.[1]

To create thin films of aluminum oxide that are decorated with surface hydroxyl groups, we studied the possibility of growing the films with water instead of oxygen. Figure 5a shows

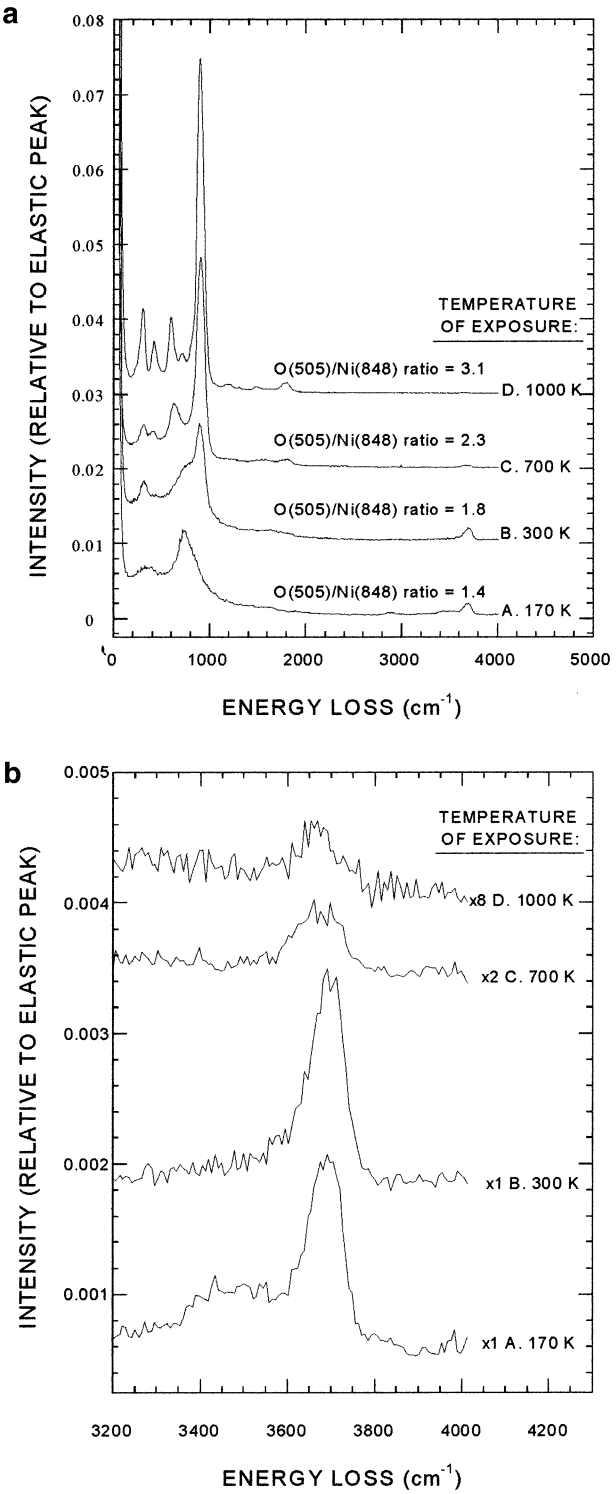

Figure 5. (a) HREELS spectra recorded after the 100 L H_2O exposure carried out on NiAl(001) at successively increasing temperatures. The Auger O(505)/Ni(848) ratio was monitored for each HREELS experiment and is indicated for the corresponding HREELS spectrum. (b) Enlargement of the hydroxyl stretching region.

HREELS spectra obtained after exposing the NiAl(001) surface to 100 L of H_2O at successively increasing temperatures. Throughout the experiments the surface composition was monitored by AES, and the O(505)/Ni(848) ratio increased linearly over the temperature range studied. Figure 5b shows an expanded view of the HREELS OH stretching region. The HREELS spectrum recorded after the 100 L H_2O exposure, carried out on NiAl(001) at 170 K, reveals the dissociative character of the water adsorption. The $\sim$300 cm^{-1} wide band, located in the $\sim$600−900 cm^{-1} energy range (peaked at 722 cm^{-1}), is due to the bending vibrations of hydroxyl groups. Another broad band, centered at 3470 cm^{-1} is assigned to the hydroxyl groups involved in extensive hydrogen bonding, which could include interactions with some molecular water on the surface. The 3690 cm^{-1} peak is assigned to the stretching vibration of an isolated hydroxyl bonded to either two or three Al atoms. Under our experimental conditions, we never observe the higher frequency (greater than 3775 cm^{-1}) OH stretch that would be associated with isolated OH groups bonded to a single aluminum atom. These assignments are based on Knössinger and Ratasnamy's work on powder samples of aluminum oxide[1] (see Figure 4) and further studies in our lab indicating at least two different types of hydroxyl groups contributing to the 3690 cm^{-1} mode.[33] The HREELS spectrum obtained after a 100 L exposure at 300 K only has an OH stretch at 3690 cm^{-1}, indicating the absence of hydrogen bonding between surface hydroxyl groups. The appearance of the $\nu_3 = 899$ cm^{-1} phonon peak following exposures at 300 K suggests the formation of surface alumina. The rest of the phonon modes of the alumina emerge in the HREELS spectra obtained after 100 L H_2O exposures at 400 K and above. The spectra recorded after 100 L H_2O exposures at 700 and 1000 K display fully developed phonon modes of γ-Al_2O_3. The additional peak at 311 cm^{-1}, that shows up strongly for the films grown at 700 and 1000 K, is assigned to the low-frequency Al−OH vibration of the surface hydroxyl against the aluminum ion. Figure 5b shows that the high-frequency OH stretching mode is present on the surfaces of thin films of alumina grown with water, regardless of growth temperature. Thus, well-ordered thin films of hydroxylated γ-Al_2O_3 can be grown on NiAl(001) by simply exposing the substrate to 100 L of H_2O within the 700−1000 K temperature range. Subsequent AES and LEED measurements showed that thin films of γ-Al_2O_3 prepared by utilizing this procedure have the same quality, thickness, and uniformity as the ones obtained by the 2400 L O_2 exposure on NiAl(001), within the same temperature range. We have also grown hydroxylated films with D_2O, and could identify the same stretching modes, appropriately shifted for the substitution of a deuterium atom for a hydrogen atom.

We also found that a hydroxylated surface could be produced by dosing a non-hydroxylated surface with water. Figure 6 shows that dosing a non-hydroxylated Al_2O_3 ultrathin film with D_2O at $T = 170$ K produces a hydroxyl (OD) stretch at 2703 cm^{-1}, which is the same frequency seen with hydroxylated films grown by exposing NiAl(001) to D_2O. On the basis of similar experiments in which we exposed the Al_2O_3 film to H_2O, we can say that molecular water is not observed under these conditions. For the FTMS experiments, this method of producing a hydroxylated surface gave more reproducible results than films grown with water.

Other research groups have used carbon monoxide to investigate the properties of powdered samples of aluminum oxide. Zaki and Knözinger examined the infrared spectra of powdered γ-Al_2O_3 exposed to CO at 80 K and found that CO would bind to hydroxyl groups on the surface. By examining how the OH stretch frequencies were affected, they found that the CO bound to only three types of hydroxyls (at 3725, 3715, and 3695 cm^{-1}). Hence, these types of hydroxyl groups are more acidic than the other hydroxyl groups.[34] Ballinger and Yates found that CO was only weakly bound to hydroxyl groups at 180 K; at 5 Torr, they could see CO bound to hydroxyl groups but not when they evacuated the chamber. They also found that

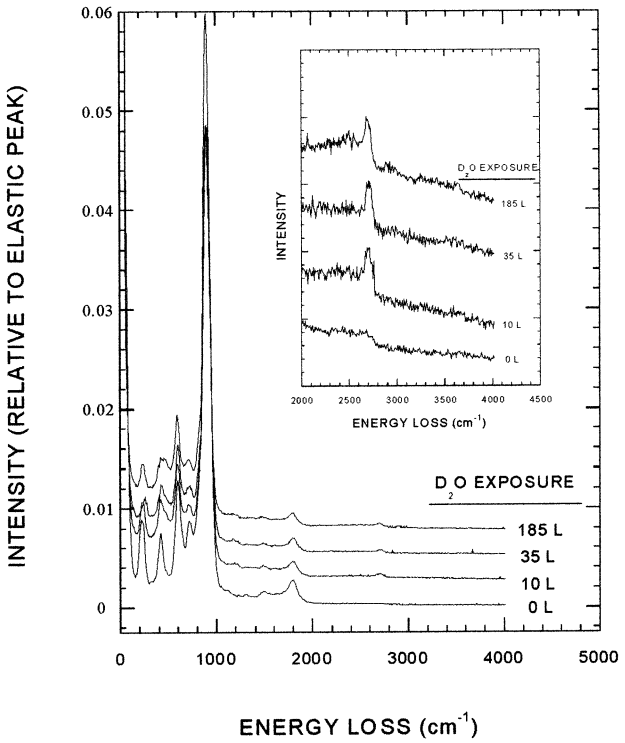

Figure 6. A HREELS spectra of hydroxylated γ-Al_2O_3, prepared by exposing a non-hydroxylated film to various amounts of D_2O at 170 K.

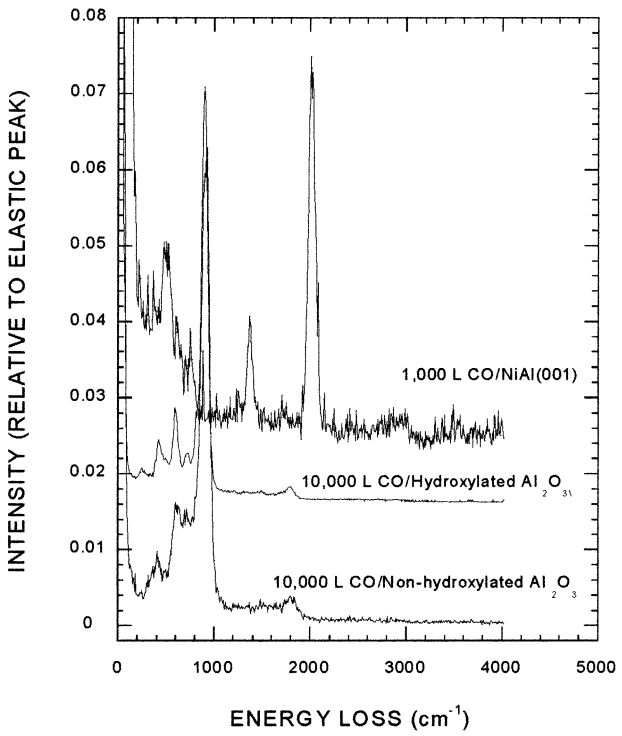

Figure 7. HREELS spectrum of CO on NiAl(001) (top spectrum). Lower two spectra show HREELS spectra of the hydroxylated and non-hydroxylated Al_2O_3 films following 10 000 L CO exposure. No indication of CO adsorption on either Al_2O_3 film is observed.

CO would bind to coordinatively unsaturated aluminum ions, giving rise to a CO stretching frequency of 2195 cm^{-1}.[35] However, CO does not bind to all coordinatively unsaturated aluminum ions; CO seems to have an affinity for only tetrahedral aluminum ions, and even then, only in particularly uncoordinated sites of multiple aluminum ions containing tetrahedral aluminum ions.[36]

To characterize the surface of our oxide thin films, we adsorbed CO on clean NiAl(001) as well as hydroyxlated and non-hydroxylated aluminum oxide at 170 K. The top spectra in Figure 7 shows that CO readily adsorbs on NiAl(001), with C−O stretching frequencies at 2009 and 1366 cm^{-1}. The stronger 2009 cm^{-1} mode is assigned to CO in an on-top site. The lower-frequency 1366 cm^{-1} mode is associated with a more strongly bonded CO that has been described as a precursor to CO dissociation on this surface.[37,38] The low-frequency mode at 511 cm^{-1} is assigned to the CO molecule−metal stretching mode. The lower two spectra in Figure 7 show that even when the hydroxylated and non-hydroxylated aluminum oxide surfaces are exposed to 10 000 L of CO at 170 K, there is no adsorbed CO. This rules out the presence of certain types of coordinatively unsaturated aluminum ions on the surface, such as the ones seen by Ballinger and Yates, but does not preclude the presence of other types of Lewis acid sites. It is not surprising that we do not see any CO bound to the hydroxyl groups at this temperature as Ballinger and Yates showed that this interaction was very weak. The absence of the $\nu_{CO} = 2009$ cm^{-1} stretching frequency on the oxide surfaces indicates that the oxide layer completely covers the NiAl surface, because any holes would expose the NiAl surface, on which CO readily adsorbs, as shown in the top spectrum of Figure 7. Given the signal-to-noise in these spectra, the amount of CO on the surface must be less than 1% of a monolayer, indicating the absence of pinholes in the oxide film at this level of surface concentration.

3.2. Chemistry of 1,3-Butadiene on NiAl(001). Figure 8 displays a set of HREELS spectra of 1,3-butadiene adsorbed

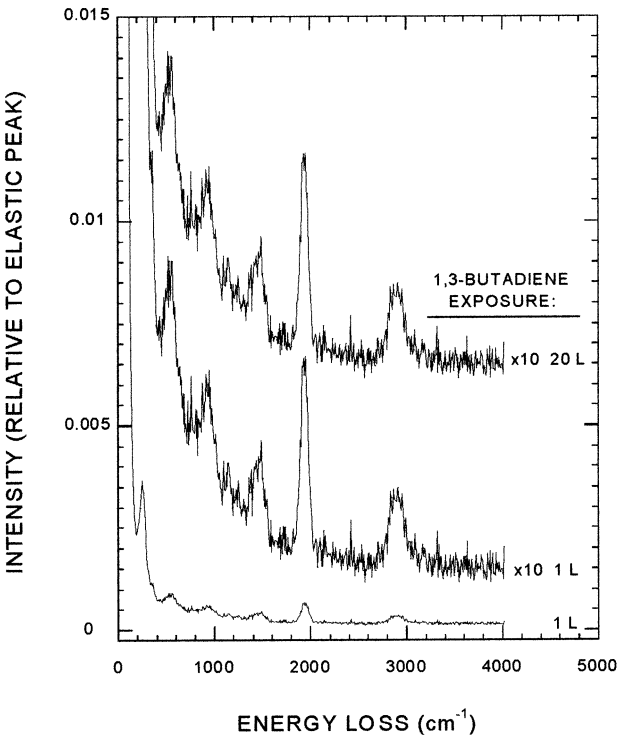

Figure 8. HREELS spectra of 1,3-butadiene adsorbed on NiAl(001) at 170 K, as a function of increasing exposure.

on NiAl(001) at 170 K as a function of increasing exposure. The AES C(272)/Ni(848) peak-to-peak ratio saturates after approximately 1 L exposure. No multilayer condensation of 1,3-butadiene was observed on NiAl(001) at 170 K. The assignment of the vibrational modes of chemisorbed 1,3-butadiene is summarized in Table 1. Vibrational modes of 1,3-butadiene adsorbed on Pt(111),[39] and normal modes of a free molecule[40]

TABLE 1: Vibrational Modes of 1,3-Butadiene

HREELS MODES (cm^{-1}) on NiAl (001) at 170 K	butadiene on Pt(111)[a]	butadiene (gas phase)[b]
243 (surface phonon)		
343 (ν_{Me-C} stretch)		
563 (CH_2 out-of-plane twist)	570	520 (δ_3 and δ_4)
774 (ν_{CC} or ν_{CH_2} rock)	780	912 ($\nu_{CC?}$)
921 (γ_{CH_2} wag)	900	1010 (δ_{vinyl})
994 (γ_{CH} out of plane or ν_{CC})	1050	1385 (δ_{CH})
1162 (CH_2 twist)	1180	
1403 (δ_{CH_2} scissors)	1430	1470 (δ_{CH_2})
1475 ($\nu_{C=C}$ stretch)		1590 ($\nu_{C=C}$)
2893 (ν_{CH} stretch)	2920, 2990, 3050	3000, 3090 (ν_{CH})

[a] Reference 39. [b] Reference 40.

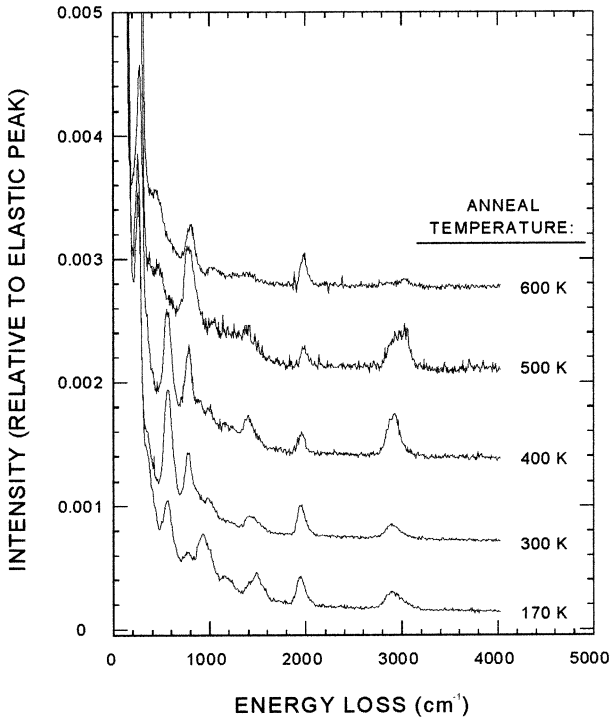

Figure 9. HREELS spectra obtained as a function of annealing temperature following 100 L exposure of 1,3-butadiene to the NiAl-(001) surface at 170 K. All spectra were obtained at 170 K.

are also shown. HREELS revealed the coverage-independent nature of the 1,3-butadiene chemisorption on NiAl(001). An $\sim$300 cm^{-1} wide asymmetric CH band at 2893 cm^{-1} appears to be significantly perturbed from its gas-phase value. Most importantly, the peak at 1475 cm^{-1} clearly indicates the presence of π-bonded 1,3-butadiene, since it falls into the appropriate $\nu_{CC} = 1450-1500$ cm^{-1} stretching region of π-bonded olefins. Hence, we conclude that at 170 K, the 1,3-butadiene is predominantly π-bonded to NiAl(001). However, the energy of the CH peak (substantially perturbed from the gas-phase frequency) suggests that the presence of some σ-bonded butadiene cannot be ruled out. The peak at 1943 cm^{-1} is due to background CO contamination, confirmed by independent HREELS measurements. This frequency is slightly lower than observed for CO adsorption on NiAl(001) by itself, due to interaction between the adsorbates on the crowded surface.[41]

Figure 9 shows a HREELS annealing experiment following a 100 L 1,3-butadiene exposure carried out on NiAl(001) at 170 K. The AES C(272)/Ni(848) ratio is $\sim$0.8 and remains fairly constant over the 170−600 K temperature range, suggesting the irreversibility of the 1,3-butadiene chemisorption on NiAl-(001). As discussed previously, the spectrum recorded after

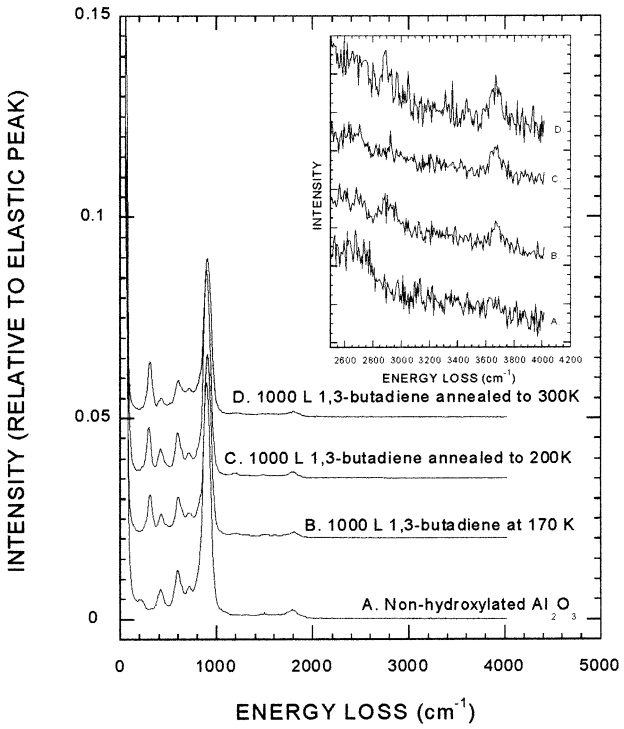

Figure 10. HREELS spectra obtained as a function of annealing temperature following 1000 L exposure of 1,3-butadiene to the non-hydroxylated Al_2O_3 surface at 170 K. All spectra were obtained at 170 K. The expanded view of the 2450−4000 cm^{-1} range is shown as an inset.

exposure at 170 K reflects the presence of primarily π-bonded 1,3-butadiene ($\nu_{CC} = 1483$ cm^{-1}). The relatively higher intensity of the CH_2 out-of-plane deformation modes (563 cm^{-1}) over in-plane modes of π-bonded butadiene implies a nearly flat adsorption geometry of the molecule. Important changes occur upon heating the substrate to 300 K. The $\nu_{CC} = 1483$ cm^{-1} stretching mode is significantly reduced in intensity, reflecting conversion of π-bonded butadiene into a σ-bonded species. This rearrangement is exemplified by the significantly increased intensity of the 774 cm^{-1} peak and the complete disappearance of the $\gamma_{CH_2} = 921$ cm^{-1} wagging mode. However, the width of the CH band is not affected by the annealing procedure, suggesting that rearrangement of the chemisorbed species is essentially nondissociative. Upon heating to 400 K, the spectrum remains unchanged, indicating the thermal stability of the chemisorbed species within the 300−400 K temperature range. Thermal decomposition of σ-bonded butadiene is apparent upon heating the substrate to 500 K. At this point, the presence of CH_2 functional groups is somewhat ambiguous. The observed spectrum can be identified as a surface covered with an admixture of $C_2H_{(ads)}$ and $CH_{(ads)}$ species. The peaks at 774 and $\sim$1381 cm^{-1} are assigned to the CH out-of-plane and in-plane bending modes, respectively, while the peak at 1023 cm^{-1} indicates the presence of intact C—C bonds. The peak at 1973 cm^{-1} is the ν_{CO} stretching modes of background CO. The HREELS spectrum recorded after heating the substrate to 600 K reflects dehydrogenation of residual hydrocarbon species.

3.3. Chemistry of 1,3-Butadiene on γ-Al_2O_3. Finally, we discuss the adsorption and reaction of 1,3-butadiene on hydroxylated and non-hydroxylated thin films of γ-Al_2O_3. Figure 10 shows a HREELS annealing experiment following a 1000 L 1,3-butadiene exposure carried out at 170 K on non-hydroxylated γ-Al_2O_3. Figure 10a corresponds to a thin film of γ-Al_2O_3 prepared by 2400 L O_2 exposure on NiAl(001) at 1000

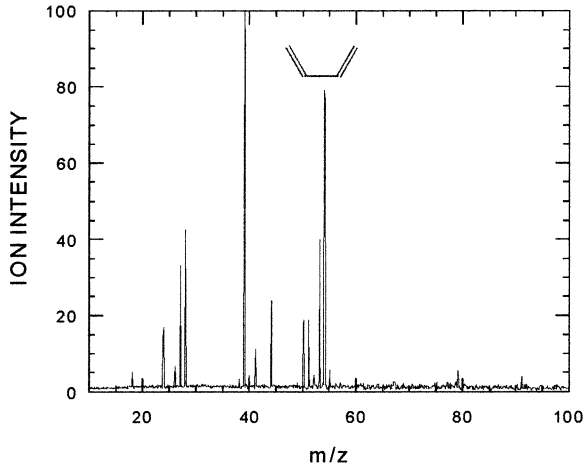

Figure 11. LID-FTMS spectrum of 1,3-butadiene on a non-hydroxylated thin film of γ-Al_2O_3 at 150 K.

K. Very strong phonon modes of γ-Al_2O_3 make the 0−1000 cm^{-1} energy range of the HREELS spectra rather inaccessible for purposes of identification of adspecies. Hence, the expanded view of the 2450−4000 cm^{-1} range, shown as an inset in Figure 10, serves as a "fingerprint" region. Figure 10b was recorded after a 1000 L 1,3-butadiene exposure carried out at 170 K on a freshly prepared thin film of γ-Al_2O_3. The $\nu_{CH} = 2901$ cm^{-1} stretching mode appears to be significantly red-shifted from the gas-phase value of a free molecule. The $\nu_{OH} = 3682$ cm^{-1} stretching mode was also present in the spectrum, indicative of at least some CH bond decomposition. The 311 cm^{-1} mode assigned to the Al−OH vibration (see the previous discussion of Figure 5) is also consistent with OH formation associated with some CH bond breaking. For 1000 L of butadiene on non-hydroxylated γ-Al_20_3, the AES C(272)/Ni(848) peak-to-peak ratio of 0.02 corresponds only to ~3% of a saturation coverage of 1,3-butadiene on clean NiAl(001). The ν_{CH} stretching mode disappeared upon warming the substrate to 200 K. AES measurements showed that the amount of surface carbon decreases with increased annealing temperature, suggesting that butadiene adsorption on non-hydroxylated γ-Al_2O_3 is partly reversible. However, as a result of the complexity of the AES process of weakly bonded species, relative changes in the adsorbate coverage cannot be determined reliably from AES measurements alone. The OH stretch remained on the substrate after annealing the sample to 300 K. Analogous results were observed for butadiene adsorbed on a hydroxylated thin film grown by exposing a NiAl(001) surface to D_2O. Similar to the non-hydroxylated surface, the presence of a $\nu_{OH} = 3675$ cm^{-1} stretch indicated that some decomposition had occurred and AES indicated that ~4% of saturation coverage of butadiene on NiAl-(001) was present. As on the non-hydroxylated surface, upon warming to 200 K, the CH band disappeared, indicating that the butadiene adsorption was largely reversible. The peaks at $\nu_{OH} = 3675$ $cm^{-1}$and $\nu_{OD} = 2703$ cm^{-1} are not affected by the annealing procedure. No H to D exchange was observed in HREELS on surfaces throughout the experiments (i.e., no CD modes were observed when butadiene was adsorbed on the surface with OD groups).

Figure 11 shows the LID-FTMS spectra following a 800 L exposure of 1,3-butadiene on non-hydroxylated aluminum oxide at 150 K. The lack of peaks at masses higher than the parent peak for butadiene ($m/z = 54$) indicates that no reaction has taken place. The cracking pattern is consistent with the gas-phase spectra for butadiene.[42] The peak at $m/z = 44$ is due to CO_2, which has a high affinity for the aluminum oxide surface

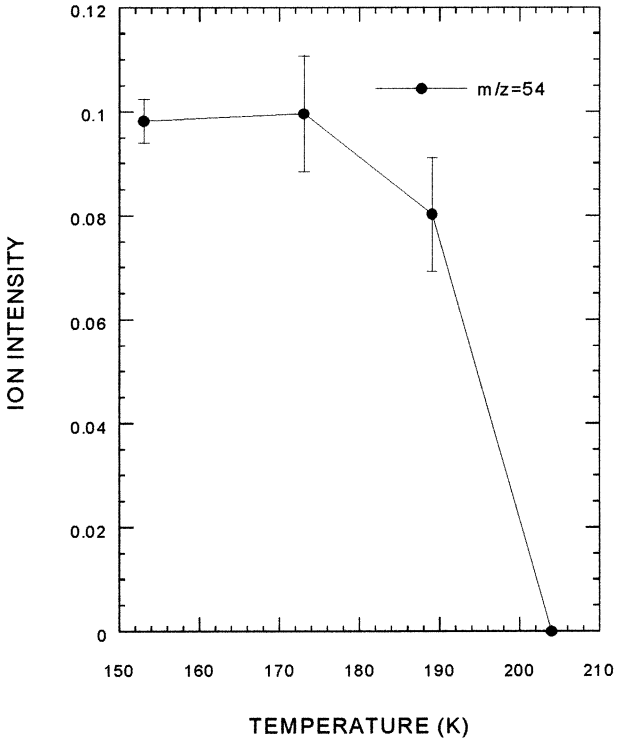

Figure 12. Mass 54 intensity (1,3-butadiene parent ion) from LID-FTMS spectra as a function of annealing temperature following adsorption on an non-hydroxylated thin film of γ-Al_2O_3. All spectra were obtained at 150 K.

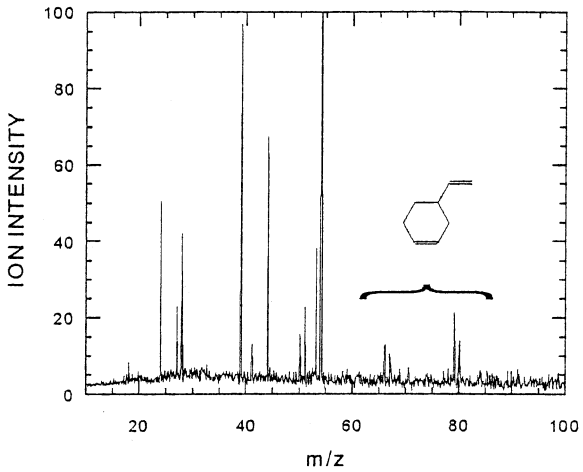

Figure 13. LID-FTMS spectrum of 1,3-butadiene on a hydroxylated thin film of γ-Al_2O_3 at 150 K. The additional peaks at $m/z = 66$, 67, 79, and 80 are characteristic of 4-vinyl-cyclohexene.

and appears in all of our LID/FTMS spectra of aluminum oxide. Figure 12 shows the parent mass 54 peak as a function of sample annealing temperature, indicating that the butadiene is only weakly bonded to the surface, desorbing by 200 K. For each data point, the sample was heated at the given temperature for two minutes. The sample was then allowed to cool, and three LID-FTMS spectra were obtained at ~150 K.

The mass spectrum obtained by laser desorption of butadiene from hydroxylated aluminum oxide (Figure 13) shows four additional peaks ($m/z = 66$, 67, 79, 80) that were not present in the spectrum of butadiene on the non-hydroxylated surface. The presence of the $m/z = 66$ cracking fragment helped identify the reaction product as 4-vinyl-cyclohexene, a dimer of butadiene. Many hydrocarbons have a cracking fragment at $m/z = 65$, but 4-vinyl-cyclohexene is the only potential product that

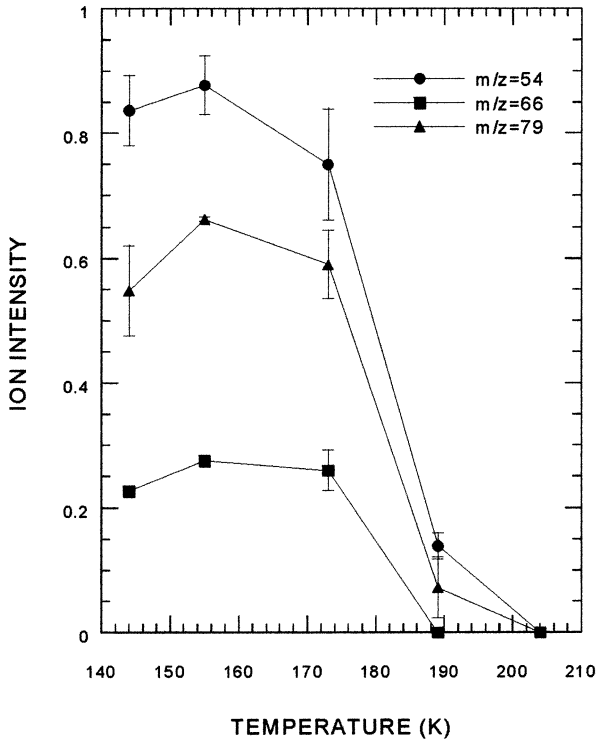

Figure 14. LID-FTMS ion intensities for 1,3-butadiene ($m/z = 54$) and 4-vinyl-cyclohexene ($m/z = 66$, 79) as a function of anneal temperature following 1,3-butadiene exposure to the hydroxylated Al_2O_3 thin film. All spectra were obtained at 150 K.

has a $m/z = 66$ peak. The parent ion of 4-vinyl-cyclohexene ($m/z = 108$) is not seen in the spectra of butadiene on hydroxylated aluminum oxide. This is to be expected because the gas-phase spectrum of 4-vinyl-cyclohexene shows that the parent peak is less than 10% of the $m/z = 79$ ion, which is the predominant cracking fragment of 4-vinyl-cyclohexene.[42] The spectra of 4-vinyl-cyclohexene also contains $m/z = 54$ and 39 as cracking fragments. Therefore these peaks in the butadiene/hydroxylated Al_2O_3 spectra are due to both 4-vinyl-cyclohexene and unreacted butadiene.

The temperature dependence of butadiene and 4-vinyl-cyclohexene was probed in the same manner as was the non-hydroxylated surface. The results, shown in Figure 14, indicate that both molecules are weakly bonded to the surface and have desorbed by 200 K. No new reaction products were seen at higher temperatures.

The dimerization of butadiene takes place only on the hydroxylated surface, so therefore the hydroxyl groups must play an important role. At the conditions employed here, we only observe one hydroxyl stretching frequency, which we have assigned as an isolated hydroxyl group tetrahedrally bonded to two or three aluminum atoms.[1,33] Zaki and Knözinger later showed by low-temperature CO experiments that these types of hydroxyl group are more acidic than hydroxyl groups bonded to fewer aluminum atoms.[34] It is possible that the dimerization of butadiene is facilitated by first one butadiene molecule being protonated by one of the Brønsted acid sites. The resulting ion could then react with another butadiene, which would then undergo ring closure and the ejection of a proton. This scenario is unlikely because the hydroxyl groups have been shown to be relatively weak acids.[43] However, to test this mechanism, we created a hydroxylated surface by dosing a non-hydroxylated surface with D_2O. Exposing this surface to butadiene showed that 4-vinyl-cyclohexene was formed, yielding a FTMS spectrum that was essentially the same as when the hydroxylated surface was grown with H_2O. If the dimerization occurred via the surface hydroxyl groups protonating the butadiene, we would expect a deuterium atom to be incorporated into the dimer, yielding *deuterated* 4-vinyl-cyclohexene as the product. This was never observed.

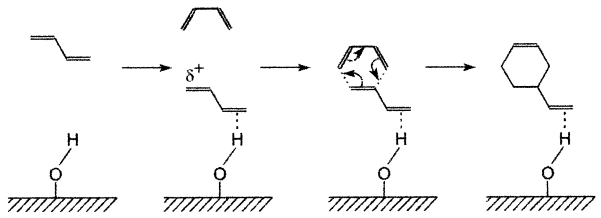

Figure 15. Proposed Diels−Alder mechanism for the formation of 4-vinyl-cyclohexene from 1,3-butadiene on hydroxylated Al_2O_3.

We therefore propose a second mechanism (see Figure 15), in which a butadiene molecule is weakly coordinated to a Brønsted acid site, which withdraws electron density from the other double bond. This activates the double bond and makes it a stronger dienophile than butadiene not associated with one of these sites. The butadiene then reacts with a gas-phase butadiene molecule in a Diels−Alder reaction, where the molecules react in a concerted fashion, producing a 4-vinyl-cyclohexene molecule that is weakly attached to the surface. The second butadiene molecule could be one from the gas phase or one that is coadsorbed on the surface prior to reaction. Our experiments do not distinguish these two possibilities. Upon heating, the molecules (product and unreacted butadiene) desorb before they have a chance to react further. When the surface is decorated with OD groups, the molecules are only weakly coordinated with the surface OD when cycloaddition occurs. Thus, there is no opportunity for deuterium incorporation into the product. Additional support for such a mechanism comes from the literature on the chemistry of powdered γ-Al_2O_3. Powdered γ-alumina has been used to catalyze Diels−Alder reactions. The presence of the alumina often serves to make the reaction more selective than the same reaction run in solvent.[44−48]

4. Summary

Thin films of aluminum oxide grown on the NiAl(001) surface are a good model for alumina catalysts and catalyst supports. These films are easily prepared and studied under UHV conditions; we have used HREELS, LEED, and AES to characterize thin films of hydroxylated and non-hydroxylated aluminum oxide under various growth conditions. Growth, which is easily controlled and repeatable, is complex, involving aluminum diffusion to the NiAl/Al_2O_3 interface and the formation of nickel-rich layers in the near-surface region. This leads to the growth dependence on the oxygen flux that we observe.

HREELS has been used to study 1,3-butadiene adsorption on three different surfaces: the NiAl(001) clean surface, hydroxylated alumina, and non-hydroxylated alumina. On the NiAl(001) surface, 1,3-butadiene is π-bonded to the surface until the substrate is heated to 300 K, above which the butadiene converts to a σ-bonded structure. On this surface, at temperatures above 400 K, the butadiene undergoes decomposition. On the hydroxylated aluminum oxide surface the 1,3-butadiene adsorption was largely reversible, although there was evidence (OH formation) for a small amount of decomposition at temperatures as low as 170 K. It was not until we used LID-FTMS experiments to examine the chemistry of butadiene on the aluminum oxide surfaces that we could see a striking difference between butadiene chemistry on the hydroxylated and non-

hydroxylated alumina surfaces. On the hydroxylated alumina surfaces the LID-FTMS experiments show that 1,2-butadiene dimerizes to form 4-vinylcylcohexene, which also desorbs from the surface molecularly.

We have shown that we can produce surface OH groups[49] on the ultrathin Al_2O_3 films on NiAl(001) that are expected to play an important role in catalytic activity. Using vibrational spectroscopy we have identified the hydroxyl groups present on our thin films as isolated hydroxyl groups. On powdered aluminum oxide, vibrational spectroscopy indicates the presence of five different isolated hydroxyl groups, as well as hydrogen-bonded hydroxyl groups.[1] On our thin films, we never see hydrogen-bonded hydroxyl groups or isolated OH groups bonded to only one aluminum ion. On bulk alumina, it is difficult to identify the specific hydroxyl group that is necessary for a given reaction to occur. The surface hydroxyl composition of bulk alumina can vary greatly, depending on the humidity and preparation condition. We have the ability to produce thin films of alumina that have a reproducible hydroxyl composition that contains only a subset of the OH groups present on bulk aluminum oxide. We plan to use these well-characterized thin films to better understand the chemistry that occurs on the hydroxyl groups of bulk aluminum oxide.

Hydroxyl groups play an important role in the dimerization of 1,3-butadiene to form 4-vinyl-cyclohexene. This chemistry does not occur on the non-hydroxylated film, which is identical to the hydroxylated alumina, other than the absence of hydroxyl groups. Therefore, we have been able to rule out the possibility of the chemistry occurring on Lewis acid sites, which are present on both the hydroxylated and non-hydroxylated thin films. We have shown that the dimerization occurs via a Diels−Alder mechanism, where a butadiene molecule is weakly coordinated to one of the hydroxyl groups, and another butadiene molecule reacts with the coordinated species to form 4-vinyl-cyclohexene.

Acknowledgment. This work was supported by the National Science Foundation under Grant CHE-9819399. We thank H. J. Freund for numerous discussions of this work.

References and Notes

(1) Knözinger, H.; Ratnasamy, P. *Catal. Rev.— Sci. Eng.* **1978**, *17*, 31.
(2) Hightower, J. W.; Hall, W. K. *J. Catal.* **1969**, *13*, 161.
(3) Hightower, J. W.; Hall, W. K. *Trans. Faraday Soc.* **1970**, *66*, 477.
(4) Medema, J. *J. Catal.* **1975**, *37*, 91.
(5) MacIver, D. S.; Wilmot, W. H.; Bridges, J. M. *J. Catal.* **1964**, *3*, 502.
(6) Corado, A.; Kiss, A.; Knözinger, H.; Müller, H.-D. *J. Catal.* **1975**, *37*, 68.
(7) Furlong, B. K.; Hightower, J. W.; Chan, T. Y.-L.; Sarkany, A.; Guczi, L. *Appl. Catal. A: General* **1994**, *117*, 41.
(8) Kaushik, V. K.; Sivaraj, C.; Rao, P. K. *Appl. Surf. Sci.* **1991**, *51*, 27.
(9) DeVries, J. E.; Yao, H. C.; Baird, R. J.; Gandhi, H. S. *J. Catal.* **1983**, *84*, 8.
(10) Gassmann, P.; Franchy, R.; Ibach, H. *Surf. Sci.* **1994**, *319*, 95.
(11) Blum, R.-P.; Niehus, H. *Appl. Phys. A* **1998**, *66*, S529.
(12) Jaeger, R. M.; Kuhlenbeck, H.; Freund, H.-J.; Wuttig, M.; Hoffmann, W.; Franchy, R.; Ibach, H. *Surf. Sci.* **1991**, *259*, 235.
(13) Libuda, J.; Winkelmann, F.; Bäumer, M.; Freund, H.-J.; Bertrams, T.; Neddermeyer, H.; Müller, K. *Surf. Sci.* **1994**, *318*, 61.
(14) Libuda, J.; Frank, M.; Sandell, A.; Andersson, S.; Brühwiler, P. A.; Bäumer, M.; Mårtensson, N.; Freund, H.-J. *Surf. Sci.* **1997**, *384*, 106.
(15) Bäumer, M.; Freund, H.-J. *Prog. Surf. Sci.* **1999**, *61*, 127.
(16) Becker, C.; Kandler, J.; Raaf, H.; Linke, R.; Pelster, T.; Dräger, M.; Tanemura, M.; Wandlet, K. *J. Vac. Sci. Technol. A* **1998**, *16*, 1000.
(17) Crowell, J. E.; Chen, J. G.; Yates, J. T., Jr. *Surf. Sci.* **1986**, *165*, 37.
(18) Wu, M.-C.; Goodman, D. W. *J. Phys. Chem.* **1994**, *98*, 9874.
(19) Chen, P. J.; Colaianni, M. L.; Yates, J. T., Jr. *Phys. Rev. B* **1990**, *41*, 8025.
(20) Chen, P. J.; Goodman, D. W. *Surf. Sci.* **1994**, *312*, L767.
(21) Wu, Y.; Garfunkel, E.; Madey, T. E. *J. Vac. Sci. Technol. A* **1996**, *14*, 2554.
(22) Wu, Y.; Garfunkel, E.; Madey, T. E. *Surf. Sci.* **1996**, *365*, 337.
(23) Macaluso, M.; Larson, R.; Delzell, E.; Sathiakumar, N.; Hovinga, M.; Julian, J.; Muir, D.; Cole, P. *Toxicology* **1996**, *113*, 190.
(24) Ward, E. M.; Fajen, J. M.; Ruder, A. M.; Rinsky, R. A.; Halperin, W. E.; Fessler-Flesch, C. A. *Toxicology* **1996**, *113*, 157.
(25) Land, D. P.; Pettiette-Hall, C. L.; Hemminger, J. C.; McIver, R. T., Jr. *Acc. Chem Res.* **1991**, *24*, 42.
(26) Pettiette-Hall, C. L.; Land, D. P.; McIver, R. T., Jr.; Hemminger, J. C. *J. Phys. Chem.* **1990**, *94*, 1948.
(27) Land, D. P.; Wang, D. T. S.; Tai, T.-L.; Sherman, M. G.; Hemminger, J. C.; McIver, R. T., Jr. Postionization of Laser-Desorbed Neutrals for the Analysis of Molecular Adsorbates on Surfaces. In *Lasers and Mass Spectrometry*; Lubman, D. M., Ed.; Oxford University Press: New York, 1990; Chapter 7, p 157.
(28) Burgess, D., Jr.; Viswanathan, R.; Hussla, I.; Stair, P. C.; Weitz, E. *J. Chem. Phys.* **1983**, *79*, 5200.
(29) Allen, H. Fundamental Surface Processes in Heterogeneous Atmospheric Chemistry: Applications to Sea-Salt (NaCl) and Oxide Particulate Chemistry, University of California, Irvine, 1997.
(30) Gassmann, P., et al. *J. Electron Spectrosc. Relat. Phenom.* **1993**, *64/65*, 315.
(31) Levin, I.; Gemming, T.; Brandon, D. G. *Phys. Stat. Sol.* **1998**, *166*, 197.
(32) Young, B. W. A.; De Wit, J. H. W. *Solid State Ionics* **1985**, *16*, 39.
(33) Layman, K. A.; Hemminger, J. C. *J. Phys. Chem. B*, in press.
(34) Zaki, M. I.; Knözinger, H. *Mater. Chem. Phys.* **1987**, *17*, 201.
(35) Ballinger, T. H.; Yates, J. T., Jr. *Langmuir* **1991**, *7*, 3041.
(36) Morterra, C.; Magnacca, G. *Catal. Today* **1996**, *27*, 497.
(37) Shinn, N. D.; Madey, T. E. *Phys. Rev. Lett.* **1984**, *53*, 2481.
(38) Moon, D. W.; Bernasek, S. L.; Dwyer, D. J.; Gland, J. L. *J. Am. Chem. Soc.* **1985**, *107*, 4363.
(39) Avery, N. R.; Sheppard, N. *Proc. R. Soc. London A* **1986**, *405*, 27.
(40) Bartholomé, E.; Karweil, J. *Z. Physik. Chem. (B)* **1937**, *35*, 442.
(41) Franchy, R.; Wuttig, M.; Ibach, H. *Surf. Sci.* **1987**, *189/190*, 438.
(42) Heller, S. R.; Milne, G. W. A. *EPA/NIH Mass Spectral Data Base*; NSRDS-NBS 63, NIST, U.S. Dept. of Commerce, 1978.
(43) Liu, X.; Truitt, R. E. *J. Am. Chem. Soc.* **1997**, *119*, 9856.
(44) Bains, S.; Pagni, R. M.; Kabalka, G. W. *Tetrahedron Lett.* **1991**, *32*, 5663.
(45) Hondrogiannis, G.; Pagni, R. M.; Kabalka, G. W.; Anosike, P.; Kurt, R. *Tetrahedron Lett.* **1990**, *31*, 5433.
(46) Hondrogiannis, G.; Pagni, R. M.; Kabalka, G. W.; Kurt, R.; Cox, D. *Tetrahedron Lett.* **1991**, *32*, 2303.
(47) Parlar, H.; Baumann, R. *Angew. Chem., Int. Ed. Engl.* **1981**, *20*, 1014.
(48) Kabalka, G. W.; Pagni, R. M.; Bains, S.; Hondrogiannis, G.; Plesco, M.; Kurt, R.; Cox, D.; Green, J. *Tetrahedron: Asymmetry* **1991**, *2*, 1283.
(49) Ivey, M. M.; Allen, H. C.; Avoyan, A.; Martin, K. A.; Hemminger, J. C. *J. Am. Chem. Soc.* **1998**, *120*, 10980.